Section 2
ADVANCED TECHNOLOGY DEVELOPMENTS

2.A Phase Conversion of Lasers with Low-Loss Distributed Phase Plates

An essential requirement for direct-drive laser fusion is the uniform irradiation of spherical targets that are located at the far field and quasi-far field of a laser system. Uniform absorption of laser light results in reduced Rayleigh-Taylor instabilities and improved spherical convergence of the target during high-density compression. A major impediment to achieving irradiation uniformity with high-power, solid-state laser systems is the presence of hot-spot structure in each of the frequency-converted beams at the target plane. The hot-spot intensity nonuniformities are caused by spatial variations in the near-field phase front of each laser beam. The central thrust of beam-uniformity studies involves controlling the beam profile presented to the target plane. Laser phase conversion provides a means to modify a laser beam's coherence properties, thereby changing its focusing characteristics.

Distributed-phase-plate (DPP) technology, previously deployed as two-level phase plates on the OMEGA laser system,[1] has been recently developed to efficiently increase the level of irradiation uniformity on target for the OMEGA Upgrade laser system. Phase conversion using two-level DPP's had provided a center-peaked energy distribution with high-order diffraction losses. However, specific profiles, such as super-Gaussian, inverse-quadratic, or cosinusoidal, do not possess undesirable diffraction losses. Target irradiation using these desired profiles increases the energy available to the target and reduces the threat of damage to target diagnostics. However, it is simultaneously required that an insensitivity to near-field wavefront errors be maintained.

Hence, the primary goal in the design of laser phase converters is to achieve lossless, wavefront-insensitive, phase conversion that allows flexible control of the laser-beam profile.

Another important goal for irradiation-uniformity research involves controlling the power spectrum and reducing the contrast of the initial speckle modulation produced by the process of phase conversion. The focusing of a spatially (phase) coherent laser beam produces a strongly modulated focal spot that contains medium- to low-frequency hot spots. On the other hand, the focusing of a phase-converted laser beam, using DPP's, produces a circularly shaped beam with a speckle distribution that contains higher frequency modulation with correspondingly higher peak irradiance. A laser-beam power spectrum, positioned somewhere between these two extremes, may provide a time instantaneous irradiation uniformity that less efficiently seeds the Rayleigh-Taylor instability. Since the validity of this assumption remains an important question, experimental investigation of this possibility, using flexible DPP technology, is warranted.

Over the past five years, lens arrays, Fourier gratings, and other diffractive optics have been developed as improvements to the two-level DPP used on the OMEGA system. Recent theoretical calculations and experimental demonstrations have shown that a large fraction of the energy, lost at the target by the two-level DPP, can now be regained by producing multibeamlet overlap with continuous DPP's that contain either an array of lenses or a two-dimensional grating-like structure. Extensive design and analysis of a new baseline DPP have been completed for the OMEGA Upgrade laser.

Phase-Plate Modeling

The randomly assigned, binary-phase-encoded, ordered array (Fig. 55.15) has been used for the phase conversion of laser light together with various beam-smoothing schemes.[1,2] However, phase conversion with two-level DPP's is not optimized for efficient energy coupling or diffraction pattern flexibility. Previous DPP's were composed of an ordered array of transparent elements. For this variety of phase plate, the phase values of approximately 15,000 hexagons are randomly binned into two levels that differ in phase by π radians. The diffraction patterns of the hexagonal beamlets are collected and brought to focus for target irradiation. The diffracted laser light, due to each hexagonal element, observed at the focal plane of a lens resembles an Airy-disc pattern. The coherent addition of all the diffracted beamlets is also approximated by an Airy-disc pattern. The encircled-energy curve shows that only a 75% energy efficiency is obtained when the 8% intensity contour is tangentially mapped to the target.

Alternatives to the two-level binary phase plate include the lenslet array, the random phase array, the Fourier grating, as well as numerous combinations of these basic forms. Each of these phase plates can be composed of either multilevel binary structures such as the optical kinoform[3] or a continuous-surface relief. In contrast to the two-level binary phase plate, the lenslet array[4–6] operates on a different principle. The lenslet array separates an incident laser beam into an array of beamlets made to overlap at the target plane by a focusing optic. The individual beamlets are directly mapped to the individual

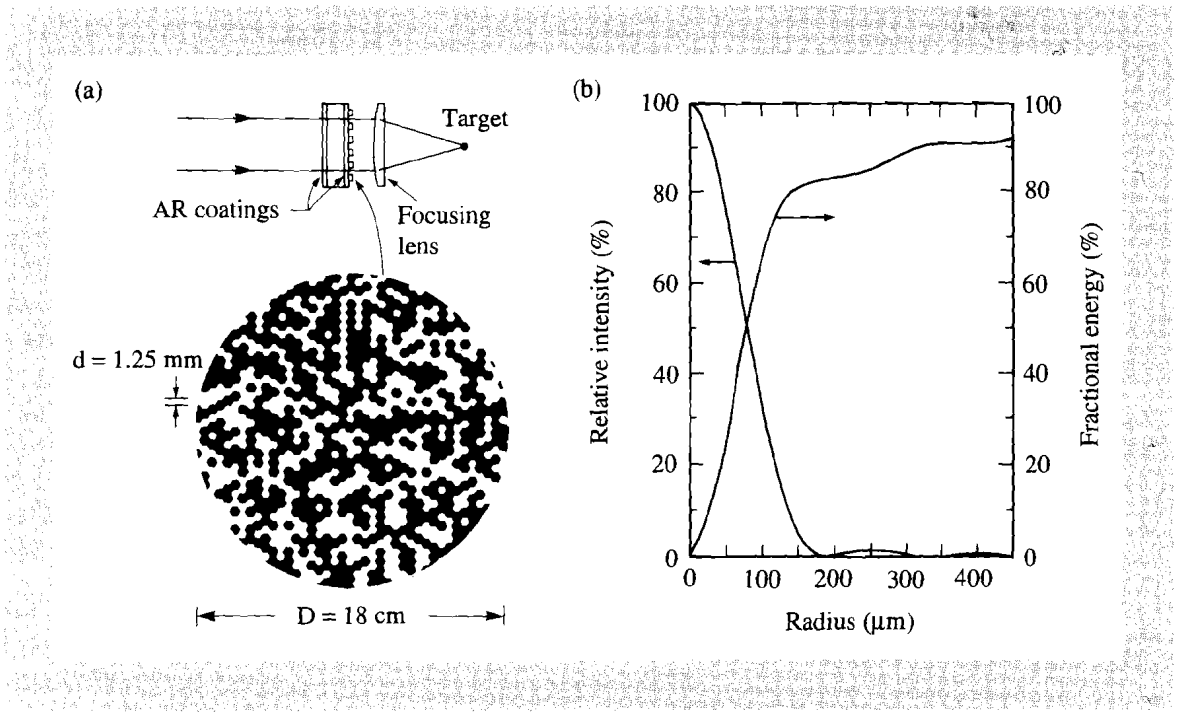

Fig. 55.15
(a) The randomly assigned, binary-phase-encoded, ordered array, referred to as a two-level distributed phase plate (DPP), was previously used for the phase conversion of the OMEGA laser to achieve smooth intensity distributions at the focal plane of a lens. Phase conversion with two-level DPP's is not optimized for energy efficiency or pattern flexibility as shown in the azimuthally averaged intensity profile (b).

elements of a Fourier plane array. Phase conversion with a lenslet array can provide high efficiency but suffers from envelope distortion and limited power spectrum flexibility. As another option for spatial phase conversion, the continuous random phase plate, characterized by a spatial correlation length and rms phase difference, uniformly increases the angular spectrum of an incident beam to form a single focal spot at the target plane. Phase conversion with a continuous random phase plate can provide high efficiency but only limited pattern flexibility.

Several new phase-plate designs are based on the simple Fourier grating.[7–13] Phase conversion with a Fourier grating can provide both high efficiency and pattern flexibility. The purpose of the Fourier grating is to diffract the collimated incident beam into multiple orders or multiple beamlets (Fig. 55.16). These orders are collected by a lens to form an array of foci at the Fourier plane of the lens. The lateral separation between the foci (d*) can be expressed in terms of the wavelength λ of light used, the *f*-number ($f_{\#}$) of the focusing lens, and the number of grooves or elements in the grating, N:

$$d^* = \lambda f_{\#} N = \lambda f N / D \ , \tag{1}$$

where N is equal to the diameter of the grating (D) divided by the groove spacing (d); $N = D/d$. The Fourier grating separates an incident laser beam into a periodic angular spectrum of beams made to focus at the focal plane of a lens. In contrast

to the lenslet array, for the case of a Fourier grating, the entire laser beam is mapped to each of the individual elements of the foci array (Fig. 55.17). Placement of the target surface outside the focal plane of the lens causes an expansion and overlap of the foci. For a system with a 28-cm-diam beam, a 1.8-m focal length, and a 700- to 1000-μm target diameter, the propagation distance beyond the focal plane (Δz) is between 0 and 4 mm. The interference pattern associated with the overlap of the beamlets depends primarily on the phase-transfer-function of the distributed phase plate.

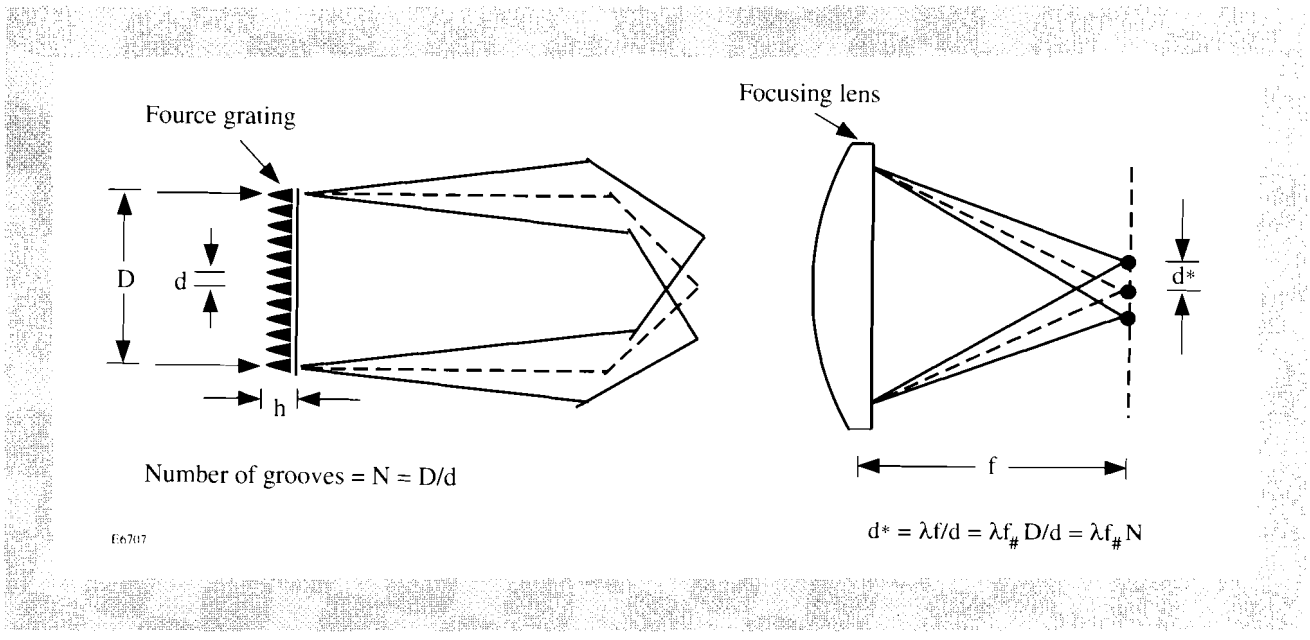

Fig. 55.16
A Fourier grating separates an incident laser beam into a periodic angular spectrum of beams brought together at the focal plane of a lens. The entire near field of the laser beam is simultaneously mapped to each of the elements of the foci array. Phase conversion with properly modified Fourier gratings can provide high efficiency and pattern flexibility.

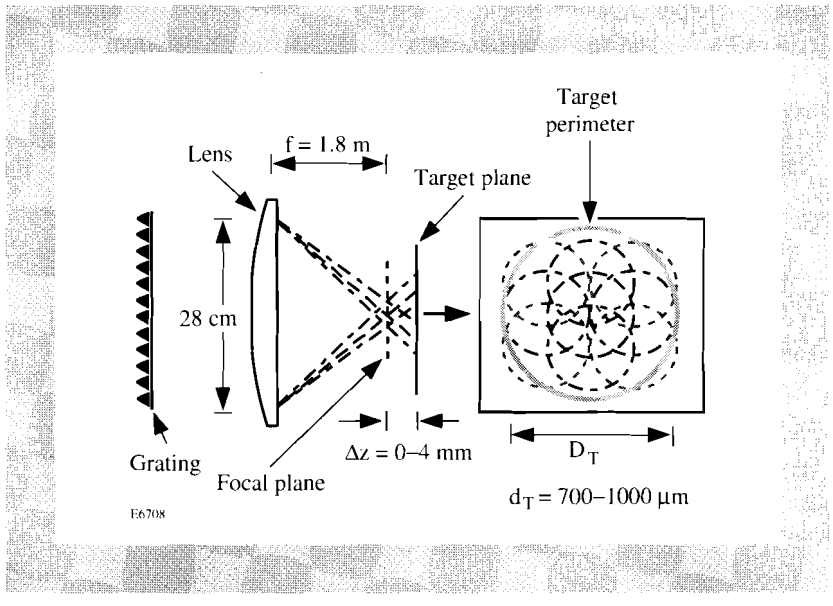

Fig. 55.17
The foci produced by a Fourier grating expand and overlap outside the focal plane of the lens. For a system with a 28-cm-diam beam, a 1.8-m focal length, and a 700- to 1000-μm target diameter, the required propagation distance beyond the focal plane is approximately 4 mm.

The profile of a surface-relief Fourier grating, schematically represented in Fig. 55.18, can in the simplest case be composed of one sinusoidal component. This simple form does not generally meet the important requirements for phase conversion; however, it is useful in explaining the basic physics of continous phase plates. Phase retardation is distributed over a two-dimensional surface by introducing optical path differences (OPD's) in the form of a thin film of varying thickness $t(x,y)$ and material refractive index n. The exact amount of phase retardation Φ experienced by a transmitted wavefront depends upon the wavelength (λ) of light and is given by

$$\phi = \frac{2\pi}{\lambda}(\mathrm{OPD}) = \frac{2\pi}{\lambda}\left[t(x,y)(n-1)\right] . \tag{2}$$

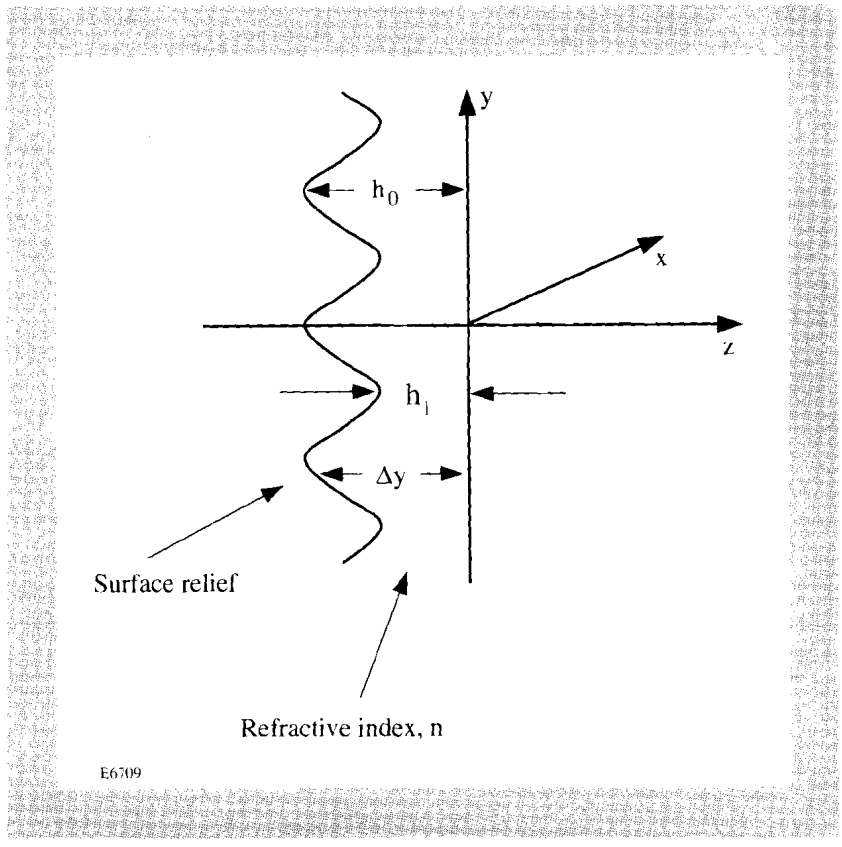

Fig. 55.18
The optical path profile of a surface-relief diffractive structure is characterized by its spatially varying surface height (thickness t) and its material index of refraction (n). These phase plates typically have a height variation of several microns and a spatial scale of several millimeters.

The complex amplitude transmittance of the two-dimensional Fourier grating is defined as

$$t(\alpha,\beta) = e^{i2kh_0} e^{ik(n-1)\left\{\left[(h_0-h_1)\cos(2\pi\alpha/d)+(h_0+h_1)\right]/2\right\}}$$

$$\times\, e^{ik(n-1)\left\{\left[(h_0-h_1)\cos(2\pi\beta/d)+(h_0+h_1)\right]/2\right\}} . \tag{3}$$

The complex amplitude distribution of the laser beam, prior to being transmitted through the phase plate, is given by

$$a_L(\alpha,\beta) = \Psi_L(\alpha,\beta) e^{i\Phi_L(\alpha,\beta)} , \tag{4}$$

where L designates the laser beam.

The amplitude distribution of the laser light after transmission through the mask is a product of Eqs. (3) and (4):

$$a(\alpha,\beta) = a_L(\alpha,\beta)t(\alpha,\beta)$$

$$= \Psi_L(\alpha,\beta)e^{i\Phi_L(\alpha,\beta)} \cdot e^{i2kh_o} e^{ik(n-1)\left\{\left[(h_o-h_1)\cos(2\pi\alpha/d)+(h_o+h_1)\right]/2\right\}}$$

$$\times e^{ik(n-1)\left\{\left[(h_o-h_1)\cos(2\pi\beta/d)+(h_o+h_1)\right]/2\right\}} . \qquad (5)$$

Sinusoidal phase modulation within the exponent gives rise to a series of Bessel functions that, in the case of a solid-state laser beam, correspond to a series of aberrated point-spread functions that exist at the focus of a lens:

$$a(\alpha,\beta) = \Psi_L(\alpha,\beta)e^{i\Phi_L(\alpha,\beta)} \cdot e^{i2kh_o} e^{i2k(n-1)(h_o+h_1)/2}$$

$$\sum_l i^l J_l\left[k(n-1)(h_o-h_1)/2\right]e^{il2\pi\alpha/d} rect(\alpha/Nd)$$

$$\sum_m i^m J_m\left[k(n-1)(h_o-h_1)/2\right]e^{im2\pi\beta/d} rect(\beta/Nd) . \qquad (6)$$

The resulting amplitude distribution located at the focal plane of a lens is given by the Fourier transform relation,

$$A(\varepsilon,\eta) = \frac{e^{i2kf}}{i\lambda f}\int\int a(\alpha,\beta)e^{-i2\pi(\alpha\varepsilon+\beta\eta)}d\alpha d\beta , \qquad (7)$$

where $a(\alpha,\beta)$ is the complex amplitude distribution and $\varepsilon = \alpha/\lambda f, \eta = \beta/\lambda f$ are the spatial-frequency variables. The input amplitude is a product of the laser-beam amplitude and the amplitude transmittance of the DPP.

Since the transform of a product is equal to the convolution of the individual transforms, $A(\varepsilon,\eta)$ can be conveniently expressed as

$$A(\varepsilon,\eta) = A_L(\varepsilon,\eta) ** N^2 d^2\left(e^{i2kf}/i\lambda f\right)e^{i2kh_o} e^{ik(n-1)(h_o+h_1)}$$

$$\sum_l i^l J_l\left[k(n-1)(h_o-h_1)/2\right]\mathrm{sinc}\left[(l/d-\varepsilon)Nd\right]$$

$$\sum_m i^m J_m\left[k(n-1)(h_o-h_1)/2\right]\mathrm{sinc}\left[(m/d-\eta)Nd\right] , \qquad (8)$$

where $A_L(\varepsilon,\eta)$ is the Fourier transform of the laser-beam amplitude.

The above expression represents a two-dimensional convolution (denoted by **) between the far-field amplitude distribution of the laser beam, $A_L(\varepsilon,\eta)$, and the individual series components. This expression indicates the effect that the laser beam has on each individual Fourier component.

The focal irradiance distribution located at the Fourier plane of a lens is given by

$$I(\varepsilon,\eta) = |A(\varepsilon,\eta)|^2$$

$$\propto \left| A_L(\varepsilon,\eta) ** \sum_l i^l J_l\left[k(n-1)(h_o - h_1)/2\right]\mathrm{sinc}\left[(l/d-\varepsilon)Nd\right] \right.$$

$$\left. \times \sum_m i^m J_m\left[k(n-1)(h_o - h_1)/2\right]\mathrm{sinc}\left[(m/d-\eta)Nd\right] \right|^2 . \qquad (9)$$

The array of foci, representing the Bessel function series associated with sinusoidal phase modulation, is shown in Figs. 55.19(a) and 55.19(b). This irradiance distribution is itself not useful for laser-fusion experiments; however, accurate control of its power spectrum is important and can, in part, be achieved by specifying a particular set of Fourier components. Non-sinusoidal spatial phase modulation is required to achieve the desired intensity pattern flexibility on target. A DPP can be designed using one of many iterative phase retrieval algorithms.[14–17] However, optimum phase plates can also be designed using specific analytic functions that represent the beam's phase. This latter approach best utilizes Fourier-intuition and experimental ingenuity. Computationally intensive iterative algorithms can then be used to complete a specific DPP design after the basic concept is established.

A continuous DPP can consist of a specific combination of a Fourier grating plus a continuous random phase plate to achieve both high efficiency and pattern flexibility at the target plane (Fig. 55.20). Phase conversion with a continuous DPP can meet these design requirements over a sufficiently long depth of focus to accommodate a wide range of target diameters. Phase-plate designs consisting of a Fourier grating together with a continuous random phase distribution can produce desirable envelopes. The irradiance distribution from the combined phase plate, as described by a cross-section through the center [Fig. 55.21(a)] and a false, three-dimensional representation [Fig. 55.21(b)], looks qualitatively similar to that of the continuous random phase plate but it is less center-peaked. The random irradiance variations associated with speckle, which obeys negative exponential statistics, is the dominant visual characteristic for both of these phase plates. In both of these cases an energy transfer greater than 95% is delivered to the target plane. The combined phase plate produces a focal spot that encircles a 700-μm target with an intensity contour of approximately 8% of the peak irradiance. Adjustments in the shape of the envelope at its center and edge

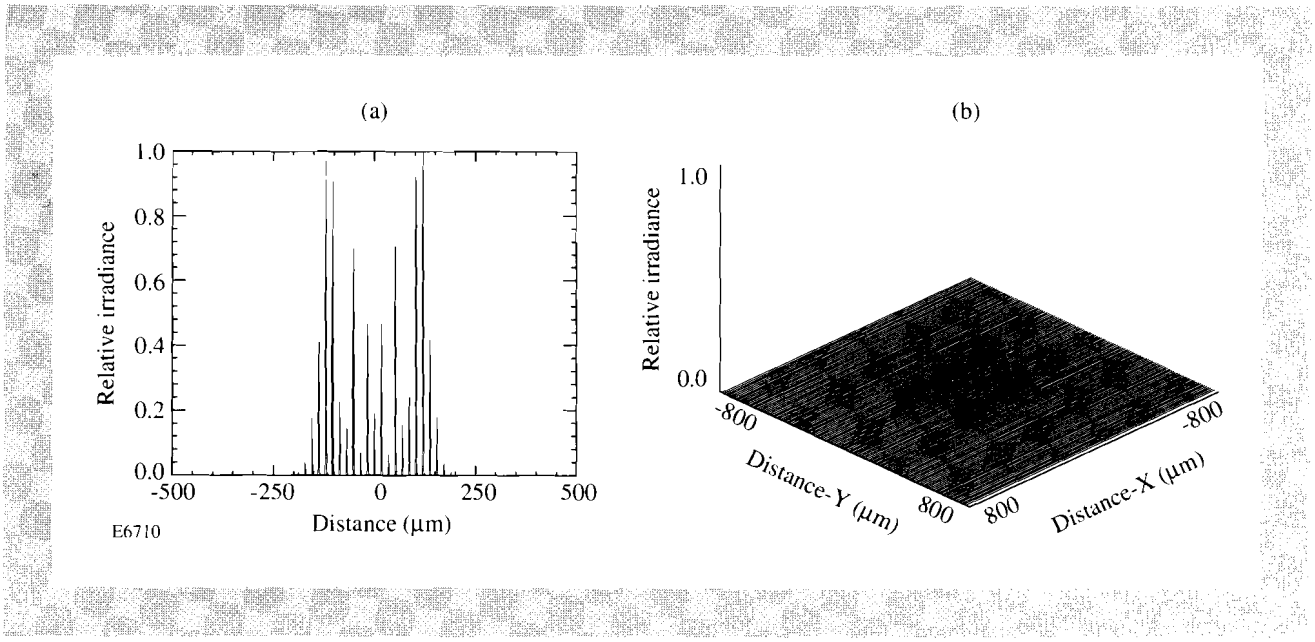

Fig. 55.19
The irradiance distribution at the focal plane of a lens contains an array of foci representing the Bessel function series associated with sinusoidal phase modulation. Figure 55.19(a) shows an intensity cross section while Fig. 55.19(b) shows the full two-dimensional distribution. This distribution is used for first-order DPP design but in itself is not useful for laser-fusion experiments. Nonsinusoidal spatial phase modulation is required to achieve the desired intensity pattern flexibility on target.

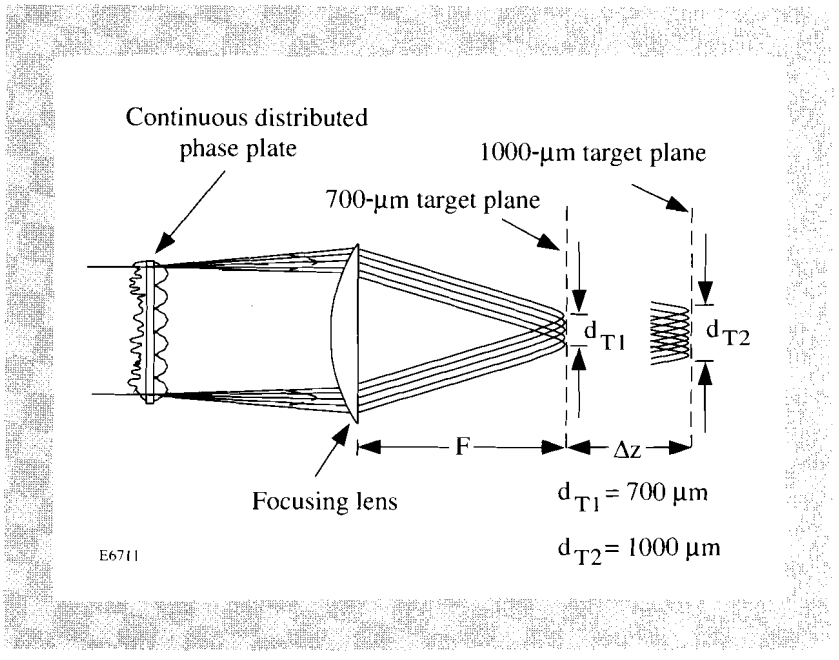

Fig. 55.20
A continuous DPP can consist of a combination of a Fourier grating and a continuous random phase plate to achieve both high efficiency and pattern flexibility at the target plane. Efficient phase conversion with a continuous DPP can be achieved over a sufficiently long depth of focus to accommodate a wide range of target diameters.

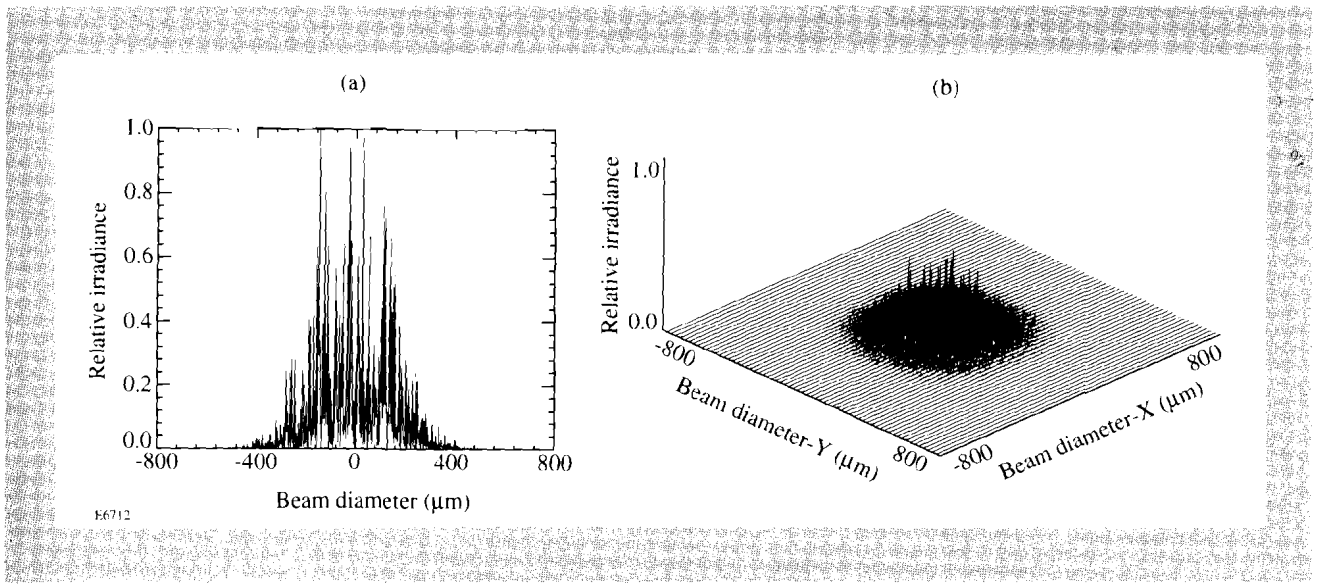

Fig. 55.21
The irradiance distribution from a continuous DPP, as described by a cross-sectional intensity scan through the beam center (a) and a false 3-D representation (b), looks qualitatively similar to that produced by a continuous random phase plate. The random irradiance variations, associated with speckle that obeys negative exponential statistics, is the dominant visual characteristic for both phase plates.

are made possible by varying the rms phase and correlation length of the random phase screen and also by varying the amplitude and frequency of the Fourier grating. Irradiation of larger targets can be accomplished with this same phase plate by placing the target outside the focal plane [Figs. 55.22(a) and 55.22(b)]. A typical axial shift from the focal plane, required to irradiate a 1000-μm target, is approximately 4 mm. Figure 55.23 shows the azimuthally averaged, energy-normalized, intensity profiles at the focal plane (solid) and a 3-mm defocused plane (dotted). The dashed curve is an azimuthally averaged intensity profile of a Gaussian beam provided for reference. Additional modeling has shown that laser-beam phase errors, as severe as twice the OMEGA UV phase error, do not significantly alter the performance of these new continuous DPP's.

The advantage of placing the phase plate before the final focusing lens is that subsequent extraction or replacement is relatively simple. However, since diffraction occurs over the distances between the phase plate and the focusing lens and between the focusing lens and the vacuum window, high intensities can be created that potentially exceed the bulk damage threshold of the fused silica windows. For this reason, certain phase-plate designs, particularly the binary-phase variety, cannot be considered at locations prior to the focusing lens on the OMEGA Upgrade laser system. The results of diffraction calculations, shown in Figs. 55.24(a) and 55.24(b), indicate that very-low-intensity modulation is created by the continuous DPP considered for use in the OMEGA Upgrade laser. In contrast to this design achievement, the two-level binary phase plate, previously used on the OMEGA laser system, creates unacceptable high-intensity modulation. If used in future experiments, binary phase plates must be placed at the vacuum window to prevent laser damage.

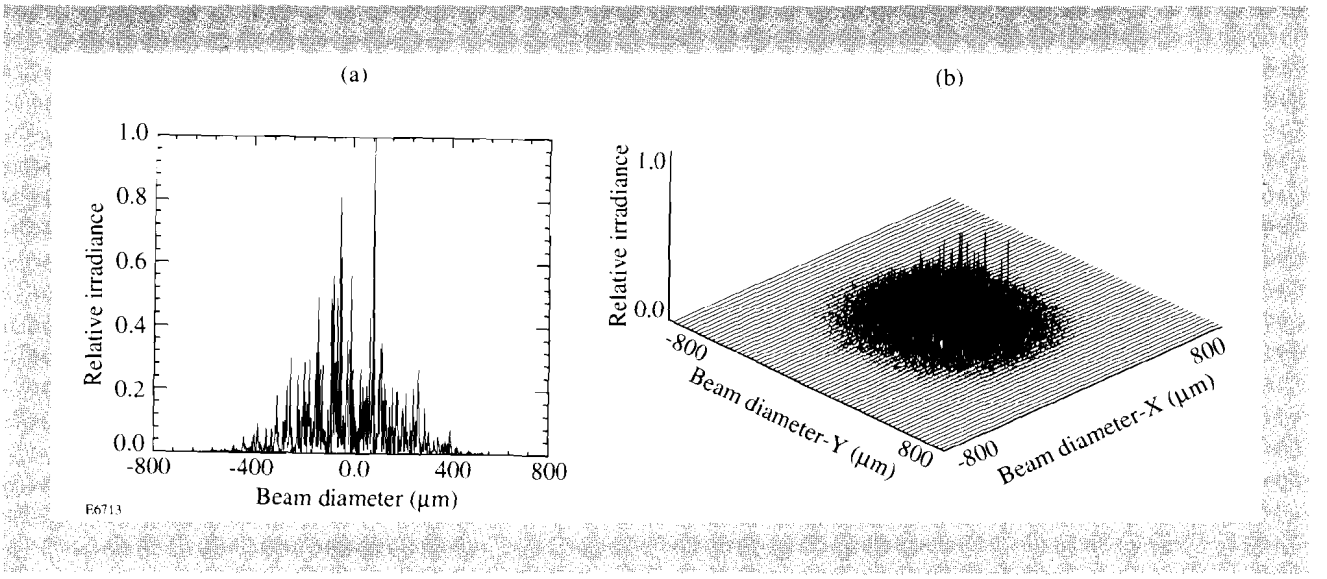

Fig. 55.22
Larger targets can be uniformly irradiated with a similar intensity envelope and speckle distribution, using the same DPP, by defocusing several millimeters along the optical axis. A cross-sectional intensity scan (a) and a 2-D intensity plot (b) illustrate the similarity to the profile obtained at the focal plane of a lens.

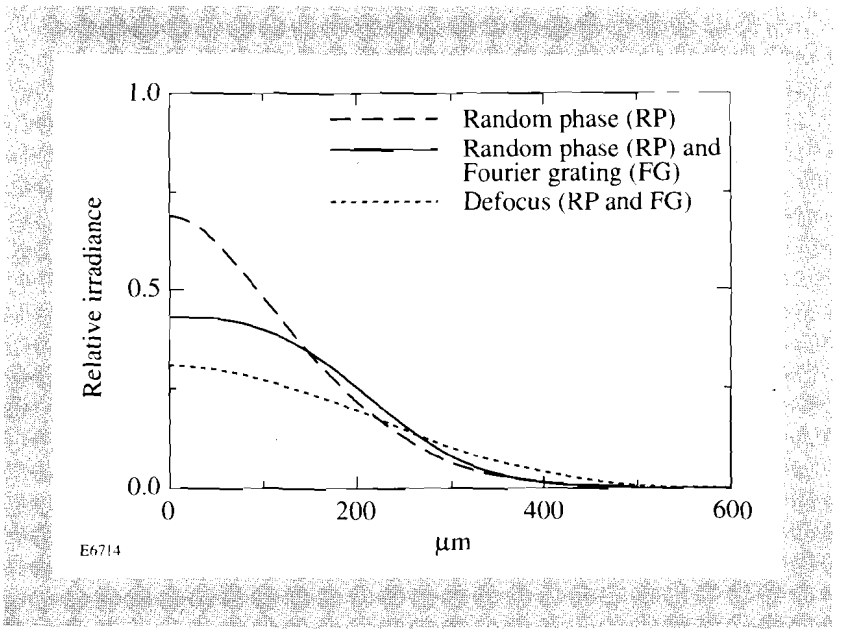

Fig. 55.23
The azimuthally averaged, energy-normalized profiles of the target-plane intensity distribution show that a DPP consisting of a Fourier grating and a continuous random phase plate (solid) is less center peaked than a Gaussian profile (dashed). Irradiation of larger targets using the same DPP is accomplished by placing the target outside the focal plane (dotted). In each case an energy transfer of 95% is delivered to the target plane.

Experimental Activities

Optical lithography has been chosen as the primary means of generating complex surface-relief structures in materials that are compatible with UV laser light. Both mask fabrication and photoresist patterning have been successfully demonstrated, using a combination of photographic and photolithographic techniques, by fabricating nearly full-scale, continuous DPP's. A major research effort at LLE currently involves the transfer and/or replication of a continuous DPP into one of the candidate UV materials. Characterization of the new DPP's involves assessment of the surface-relief transfer process and accurate measurement of the

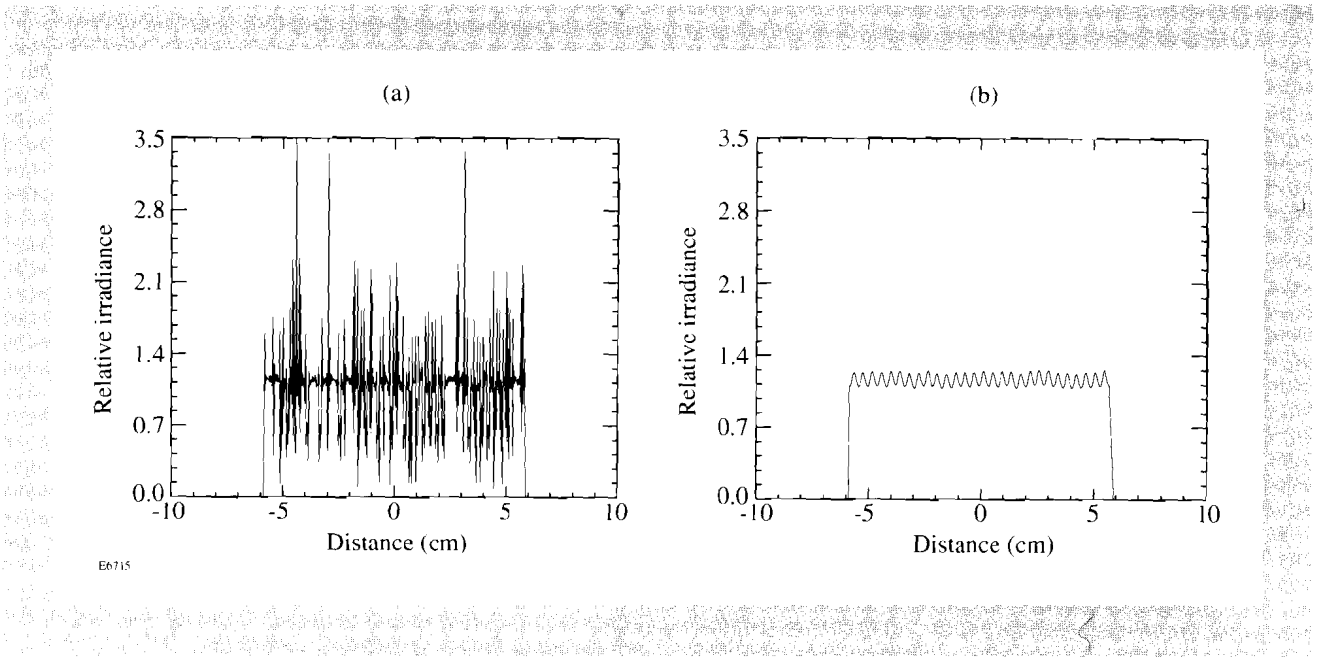

Fig. 55.24
Diffraction occurs over the distances between the phase plate, focusing lens, and vacuum window, causing high intensities that potentially exceed the bulk damage threshold of fused silica windows. The two-level binary phase plate, previously used on the OMEGA laser system, creates unacceptable high-intensity modulation (a); however, very-low-intensity modulation is created by the new continuous DPP (b).

target-plane irradiance. Experimental investigation of the effects that the new DPP has on laser-beam alignment to the target is also critical to overall performance of the phase plate. It is anticipated that future studies of target performance and irradiation uniformity will provide the necessary requirements for optimum phase conversion of the OMEGA Upgrade laser system.

Conclusions

A new variety of DPP, characterized as deep, surface-relief, continuous phase plates, has been invented for use within the OMEGA Upgrade laser system. These DPP's can perform nearly lossless phase conversion of high-power laser beams, thus delivering up to 25% more energy directly to the fusion capsule. Specific DPP designs can provide the desired intensity envelope and speckle distribution (power spectrum) over the full 700- to 1000-μm range of target diameters envisioned for the future experimental target physics program at LLE. In addition, these new phase plates offer substantially less concern for optical damage due to diffraction-induced intensity ripples in the near field of the laser beams. An extensive experimental program is now underway to fabricate and characterize large-aperture, ultraviolet, continuous DPP's. These DPP's possess both unity efficiency and high damage threshold, meeting the design requirements for the OMEGA Upgrade laser system.

ACKNOWLEDGMENT

This work was supported by the U.S. Department of Energy Office of Inertial Confinement Fusion under Cooperative Agreement No. DE-FC03-92SF19460, the University of Rochester, and the New York State Energy Research and Development Authority. The support of DOE does not constitute an endorsement by DOE of the views expressed in this article.

REFERENCES

1. LLE Review **33**, 1 (1988).
2. Y. Kato *et al.*, Phys. Rev. Lett. **53**, 1057 (1984).
3. L. B. Lesem, P. M. Hirsch, and J. A. Jordan, Jr., IBM J. Res. Develop. **13**, 150 (1969).
4. X. Deng *et al.*, Appl. Opt. **25**, 377 (1986).
5. P. Langois and R. Beaulieu, Appl. Opt. **29**, 3434 (1990).
6. T. Jitsuno *et al.*, presented at CLEO '92, paper CThI2.
7. H. Dammann and K. Görtler, Opt. Commun. **3**, 312 (1971).
8. J. Jahns *et al.*, Opt. Eng. **28**, 1267 (1989).
9. U. Krackhardt, J. N. Mait, and N. Streibl, Appl. Opt. **31**, 27 (1992).
10. N. Streibl, J. Mod. Opt. **36**, 1559 (1989).
11. D. Daly, S. M. Hodson, and M. C. Hutley, Opt. Commun. **82**, 183 (1991).
12. P. Ehbets *et al.*, Opt. Lett. **17**, 908 (1992).
13. D. Prongué *et al.*, Appl. Opt. **31**, 5706 (1992).
14. R. W. Gerchberg and W. O. Saxton, OPTIK **35**, 237 (1972).
15. J. R. Fienup, Appl. Opt. **21**, 2758 (1982).
16. K. Ichikawa, A. W. Lohmann, and M. Takeda, Appl. Opt. **27**, 3433 (1988).
17. P. E. Keller and A. F. Gmitro, submitted to Applied Optics.

2.B Nematic Polymer Liquid-Crystal Wave Plate for High-Power Lasers at 1054 nm

Liquid-crystalline materials capable of replacing traditional crystalline solids in the production of wave plates are becoming more desirable due to the high cost of the solid crystals typically used,[1] including natural and synthetic mica, quartz, sapphire, magnesium fluoride, and KDP (potassium dihydrogen phosphate). The laborious and often expensive process of high-precision optical polishing of plates fabricated from these crystals makes their use still less feasible for large-aperture requirements. In addition, the range of available retardance values is limited, and the laser-damage thresholds are not always known.

Low-molecular-weight liquid-crystal monomers (LMLC's) have overcome the cost disadvantages of typical solid crystals. LMLC's are particularly successful in meeting specific retardance needs and can exhibit high resistance to pulsed-laser damage in IR and UV regimes.[2] Despite their many successes, LMLC's introduce some difficulties of their own—the use of thick glass substrates to support the LC without bowing and the epoxy sealing of these substrates without long-term transmitted-wavefront distortion due to the sealant.[3]